

Effect of weak disorder in multi-Weyl semimetals

Zhen Ning(宁震), Bo Fu(付博), Qinwei Shi(石勤伟), Xiaoping Wang(王晓平)

Citation: Chin. Phys. B . 2020, 29(7): 077202 . **doi:** 10.1088/1674-1056/ab9612
Journal homepage: http://cpb.iphy.ac.cn; http://iopscience.iop.org/cpb

What follows is a list of articles you may be interested in

Se substitution and micro-nano-scale porosity enhancing thermoelectric Cu_2Te

Xiaoman Shi(史晓曼), Guoyu Wang(王国玉), Ruifeng Wang(王瑞峰), Xiaoyuan Zhou(周小元), Jingtao Xu(徐静涛), Jun Tang(唐军), Ran Ang(昂然)

Chin. Phys. B . 2018, 27(4): 047204 . **doi:** 10.1088/1674-1056/27/4/047204

Synthesis and thermoelectric properties of Nd-single filled p-type skutterudites

Hong Wu(吴宏), Nusrat Shaheen, Heng-Quan Yang(杨恒全), Kun-Ling Peng(彭坤岭), Xing-Chen Shen(沈星辰), Guo-Yu Wang(王国玉), Xu Lu(卢旭), Xiao-Yuan Zhou(周小元)

Chin. Phys. B . 2018, 27(4): 047203 . **doi:** 10.1088/1674-1056/27/4/047203

Optimize the thermoelectric performance of CdO ceramics by doping Zn

Xin-Yu Zha(查欣雨), Lin-Jie Gao(高琳洁), Hong-Chang Bai(白洪昌), Jiang-Long Wang(王江龙), Shu-Fang Wang(王淑芳)

Chin. Phys. B . 2017, 26(10): 107202 . **doi:** 10.1088/1674-1056/26/10/107202

Spin-valley Hall conductivity of doped ferromagnetic silicene under strain

Bahram Shirzadi, Mohsen Yarmohammadi

Chin. Phys. B . 2017, 26(1): 017203 . **doi:** 10.1088/1674-1056/26/1/017203

Alternating current characterization of nano-Pt(II) octaethylporphyrin (PtOEP) thin film as a new organic semiconductor

M Dongol, M M El-Nahass, A El-Denglawey, A A Abuelwafa, T Soga

Chin. Phys. B . 2016, 25(6): 067201 . **doi:** 10.1088/1674-1056/25/6/067201

RAPID COMMUNICATION

Effect of weak disorder in multi-Weyl semimetals*

Zhen Ning(宁震)[1], Bo Fu(付博)[2,†], Qinwei Shi(石勤伟)[3], and Xiaoping Wang(王晓平)[1,3]

[1] Department of Physics, University of Science and Technology of China, Hefei 230026, China
[2] Department of Physics, The University of Hong Kong, Hong Kong, China
[3] Hefei National Laboratory for Physical Sciences at the Microscale & Synergetic Innovation Center of Quantum Information and Quantum Physics, University of Science and Technology of China, Hefei 230026, China

(Received 5 March 2020; revised manuscript received 18 May 2020; accepted manuscript online 25 May 2020)

We study the behaviors of three-dimensional double and triple Weyl fermions in the presence of weak random potential. By performing the Wilsonian renormalization group (RG) analysis, we reveal that the quasiparticle experiences strong renormalization which leads to the modification of the density of states and quasiparticle residue. We further utilize the RG analysis to calculate the classical conductivity and show that the diffusive transport is substantially corrected due to the novel behavior of the quasiparticle and can be directly measured by experiments.

Keywords: Weyl semimetals, renormalization group, quasiparticle, conductivity

PACS: 72.80.Ng, 72.10.–d, 11.10.Gh **DOI:** 10.1088/1674-1056/ab9612

1. Introduction

Topological phases of matter with gapless low energy excitation continue to attract broad attention due to their exotic physical properties. For example, three-dimensional Weyl semimetal (WSM) refers to a class of topological materials which are characterized by isolated band touching points and the low energy excitation is described by the massless Dirac equation. Such Weyl nodes carry ± 1 topological charges and act as a monopole in the momentum space. Much recently, the linear dispersion in all three directions has been experimentally investigated in TaAs[1–3] and NbAs,[4] which provides a practical route to detect the novel phenomena associated with the emergent Weyl fermions, such as the negative magnetoresistance induced by the chiral anomaly,[5] and the anomalous Hall effect due to the nontrivial Berry curvature.[6–8] A general Weyl semimetal carries multiple monopole charges n, and the low energy quasiparticle dispersion relation is anisotropic $\varepsilon_k = \sqrt{v_z^2 k_z^2 + v_\parallel^2 k_\parallel^{2n}}$, where $k_\parallel^2 = k_x^2 + k_y^2$, the two known examples under investigation are referred to as double ($n = 2$) and triple ($n = 3$) Weyl semimetals. Possible candidates for the realization of double Weyl systems are reported in $HgCr_2Se_4$,[9,10] $SrSi_2$,[11] or in the optical lattices.[13,14] Recently, by using density functional theory, it has been pointed out that a group of molybdenum monochalcogenide compounds[12] $A(MoX)_3$ (A = Rb, Tl; X = Te) possess the property of triple Weyl fermion. The anisotropic dispersion leads to qualitative differences in many physical properties between single- and multi-Weyl semimetals. A direct consequence is that, for the multi-Weyl semimetal the transport properties display relativistic dynamics along k_z direction and non-relativistic dynamics along the other directions[18–22]. In the presence of short range[15] and Coulomb interactions,[16,17] there are many interesting physical consequences, such as anisotropic screening, exotic phase transitions, and critical behavior.

The effect of disorder, which cannot be avoided in real systems, is one of the central issues in condensed matter physics. One of the most celebrated examples is the disorder driven quantum phase transition. In single WSM, it has been widely studied by theoretical analysis[23–25] and numerical simulations.[26,27] There exists a critical strength of disorder, below which the disorder is an irrelevant perturbation and the system remains stable with weak disorder. According to the renormalization group analysis, the charge transport in Weyl semimetal obeys a novel scaling behavior in the vicinity of the quantum critical point. In contrast to the single WSM, scaling analysis[29] shows that the disorder is a marginally relevant perturbation in double WSM and a relevant perturbation in triple WSM, which indicates that the disorder acts more directly in multi WSM than in single WSM. It has been reported that the multi WSM ($n > 1$) is unstable against disorder,[28,29] and even the weak disorder can drive the system into a diffusive metal (DM) phase.

In this paper, we investigate the density of states and transport properties of weakly disordered double and triple WSMs. In the conventional metals with finite Fermi surface, the perturbative analysis is well controlled by the parameter $(E_F\tau)^{-1}$,[30–32] as long as the Fermi energy is away from the band edge, the disorder vertex correction (crossed Feynman diagrams) can be dropped out. However, in semimetal sys-

*Project supported by the National Natural Science Foundation of China (Grant No. 11874337).
†Corresponding author. E-mail: bofu123@mail.ustc.edu.cn
© 2020 Chinese Physical Society and IOP Publishing Ltd

tems such as graphene,[33,35,36] the weak disorder condition $E_F\tau \gg 1$ is no longer satisfied as the Fermi level E_F is close to the nodal point,[34,39] the results obtained under the self consistent Born approximation (SCBA)[44] are not enough and the renormalization of disorder vertex needs to be taken into account.[37–40] Indeed, the previous study of the Dirac fermion in graphene based on one-loop renormalization group (RG) shows that such interference processes give rise to the ultraviolet logarithmic corrections to the density of states and classical conductivity.[39,40] Here, we point out that similar logarithmic quasiparticle residue Z_E exists in weakly disordered double WSM, for triple WSM the logarithmic function is replaced by a cube root behavior. We further discuss the modification of the classical conductivity due to the unusual quasiparticle residue Z_E which gives significant contribution to the conductivity along the direction of linear dispersion.

2. Model and theoretical method

The low energy effective Hamiltonian which can describe the clean multi WSM is written as[19,20]

$$H_n(\boldsymbol{k}) = v_\parallel(k_-^n\sigma_+ + k_+^n\sigma_-) + v_z k_z\sigma_z, \tag{1}$$

where $k_\pm = k_x \pm k_y$, $\sigma_\pm = \frac{1}{2}(\sigma_x \pm \sigma_y)$, v_z is the effective velocity along the z direction, and $v_\parallel$ is a material-dependent constant parameter. We consider the coordinate transformation $k_x = \left(k\sin\theta/v_\perp\right)^{1/n}\cos\phi$, $k_y = \left(k\sin\theta/v_\perp\right)^{1/n}\sin\phi$, $k_z = (k/v_z)\cos\theta$, then the eigenfunction of the Hamiltonian can be written as

$$|+\rangle = \begin{pmatrix} \cos\dfrac{\theta}{2} \\ \sin\dfrac{\theta}{2}e^{in\phi} \end{pmatrix}, \quad |-\rangle = \begin{pmatrix} -\sin\dfrac{\theta}{2} \\ \cos\dfrac{\theta}{2}e^{in\phi} \end{pmatrix}. \tag{2}$$

The eigenvalues of the Hamiltonian are $\varepsilon_{k\pm} = \pm\sqrt{v_z^2k_z^2 + v_\parallel^2k_\parallel^{2n}}$, where $k_\parallel^2 = k_x^2 + k_y^2$. The quasiparticle dispersion relation is linear along the k_z axis, and is quadratic or cubic dispersion in the k_xk_y plane for double ($n=2$) or triple ($n=3$) WSM. Then, the disorder part of the Hamiltonian is described by the random potential $\hat{V} = \sum_{\boldsymbol{r}} V(\boldsymbol{r})|\boldsymbol{r}\rangle\langle\boldsymbol{r}|$, where $V(\boldsymbol{r})$ is distributed uniformly and independently in $[-W/2, W/2]$. We perform disorder averaging under the zero mean condition $\overline{V(\boldsymbol{r})} = 0$ and the correlation is given by $\overline{V(\boldsymbol{r})V(\boldsymbol{r'})} = \gamma\delta_{\boldsymbol{r}\boldsymbol{r'}}$, where $\gamma = W^2/12$. The effective action[23,29] including a disorder induced four-Fermion interaction term is

$$\begin{aligned} S = &\int \mathrm{d}\tau\mathrm{d}^3x\psi_r^\dagger(x,\tau)[\partial_\tau - H_n(\boldsymbol{r})]\psi_r(x,\tau) \\ &- \frac{\gamma}{2}\int \mathrm{d}\tau\mathrm{d}\tau'\mathrm{d}^3r(\psi_r^\dagger\psi_r)_{x,\tau}(\psi_{r'}^\dagger\psi_{r'})_{x,\tau'}, \end{aligned} \tag{3}$$

where r, r' are replica indices and the real space Hamiltonian $H_n(\boldsymbol{r})$ can be obtained by replacing the wave vector with momentum operator $\hat{\boldsymbol{k}} = -\mathrm{i}\nabla$. The notation $\psi_r^\dagger(x,\tau)\psi_r(x,\tau) \equiv (\psi_r^\dagger\psi_r)_{x,\tau}$ is used for abbreviation. Next, we perform one-loop renormalization and derive the RG flow equations for v_z, $v_\parallel$, and γ. In doing so, we have to calculate the self-energy and vertex correction by considering the one-loop Feynman diagram in Fig. 1. The propagator of the Weyl fermion is $G(E,\boldsymbol{k}) = \dfrac{1}{E - v_\parallel(k_-^n\sigma_+ - k_+^n\sigma_-) - v_zk_z\sigma_z}$, and we have

$$\begin{aligned} \text{(a)} &= \gamma\int\frac{\mathrm{d}^3k}{(2\pi)^3}G(E,\boldsymbol{k}) \\ &= \gamma I_n\int_{\Lambda e^{-l}}^{\Lambda}k^{2/n}\mathrm{d}k\frac{E}{E^2-\varepsilon_k^2} \\ &= -\gamma I_n\Lambda^{2/n-1}El, \\ \text{(b)} &= 2\gamma^2\int\frac{\mathrm{d}^3k}{(2\pi)^3}G(E,\boldsymbol{k})G(E,\boldsymbol{k}) \\ &= 2\gamma^2I_n\int_{\Lambda e^{-l}}^{\Lambda}k^{2/n}\mathrm{d}k\frac{\varepsilon_k^2}{(E^2-\varepsilon_k^2)^2} \\ &= 2\gamma(\gamma I_n\Lambda^{2/n-1})l. \end{aligned} \tag{4}$$

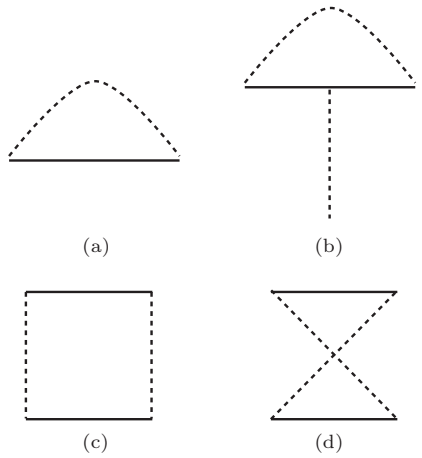


Fig. 1. One–loop Feynmann diagrams arising from disorder induced coupling (dotted lines), the solid lines represent the propagator of fermion. (a) Disorder induced fermion self-energy, (b) vertex correction, (c) ladder and (d) crossing diagrams.

We perform a shell integration in $\Lambda e^{-l} < k < \Lambda$, where Λ is the ultraviolet cut-off for energy. The ladder (Fig. 1(c)) and crossing (Fig. 1(d)) diagrams have no correction to the disorder vertex and do not contribute to the RG flow of disorder coupling. The constant I_n comes from the angle integration of the Jacobian corresponding to the coordinate transformation,

$$\begin{aligned} I_n &= \frac{1}{(2\pi)^3}\int_0^\pi\mathrm{d}\theta\int_0^{2\pi}\mathrm{d}\phi\frac{\csc\theta(\sin\theta)^{2/n}}{nv_\parallel^{2/n}v_z} \\ &= \frac{2\pi^{3/2}\Gamma(1/n)}{nv_\perp^{2/n}v_z\Gamma(1/2+1/n)(2\pi)^3}. \end{aligned} \tag{5}$$

We can redefine a dimensionless disorder coupling constant $\Delta_n = \gamma I_n\Lambda^{2/n-1}$. Then, we perform the scaling analysis of the action. Considering the anisotropy of the Hamiltonian $H_n(\boldsymbol{r})$, we take the scaling transformation as $(r_\parallel, z) \to$

$(b^{1/n}r_\parallel, bz)$, accompanied by $\tau \to b^z\tau$, where $b = e^l$, and we obtain

$$S = \int d\tau d^3x b^{z+d_n} \psi_r^\dagger(x,\tau)\left[(1+\Delta l)\partial_\tau - v_\parallel b^{-1}(\hat{k}_-^n\sigma_+ + \hat{k}_+^n\sigma_-) - b^{-1}v_z\hat{k}_z\sigma_z\right]\psi_r(x,\tau) - \frac{\gamma}{2}(1+\Delta l)\int d\tau d\tau' d^3r b^{2z+d_n}(\psi_r^\dagger\psi_r)_{x,\tau}(\psi_{r'}^\dagger\psi_{r'})_{x,\tau'}, \quad (6)$$

where we have defined the effective dimension as $d_n = 1 + 2/n$. To keep the action S invariant under scale transformation, we take $\psi \to Z_\psi^{-1/2}\psi$, where $Z_\psi = b^{d_n}(1+\Delta l)$, and we obtain the RG-flow equations

$$\frac{dv_{\parallel,z}}{dl} = (z-1-\Delta_n)v_{\parallel,z},$$
$$\frac{d\Delta_n}{dl} = (2-d_n)\Delta_n + 2\Delta_n^2. \quad (7)$$

The first term of equation Δ is dependent on the dimension of the disorder coupling $2-d_n$. For single WSM ($d_n = 3$), the dimension of Δ is negative and the disorder is irrelevant for weak disorder, which are addressed in Ref. [23]. However, the increase of the monopole charge n effectively reduces the dimension $d_n = 1+2/n$, the dimension of disorder coupling is zero for double WSM ($n = 2$, marginally relevant) and positive for triple WSM ($n = 3$, relevant), and the systems (for $n > 1$) are expected to be unstable even in the presence of weak disorder.[28,29]

The solution of the equation for Δ_n is $\Delta_2(L) = \frac{\Delta_2}{1-2\Delta_2 L}$ and $\Delta_3(L) = \frac{\Delta_3 e^{L/3}}{1+6\Delta_3(1-e^{L/3})}$. Using the relation $L \sim \ln(\Lambda/E)$,[42] we obtain

$$\Delta_2(E) = \frac{\Delta_2}{1-2\Delta_2\ln(\Lambda/E)},$$
$$\Delta_3(E) = \frac{\Delta_3(\Lambda/E)^{1/3}}{1-6\Delta_3[(\Lambda/E)^{1/3}-1]}, \quad (8)$$

where we set the initial value $\Delta_n(E=\Lambda)$ as Δ_n for simplicity. The disorder coupling is increased as the energy reduces and is divergent when $E \to E_c$. The RG flow is terminated when the energy reaches the low energy cut off E_c,

$$E_c^{(n=2)} = \Lambda e^{-\frac{1}{2\Delta_2}}, \quad E_c^{(n=3)} = \Lambda\left(\frac{6\Delta_3}{1+6\Delta_3}\right)^3. \quad (9)$$

By defining the dynamic exponent $z = 1+\Delta_n$,[23] the flow equation of $v_{\parallel,z}$ is fixed. In the rest of the paper, we will discuss the renormalization of density of states and classical conductivity using the renormalization of disorder coupling $\Delta_n(E)$.

3. Density of states

In this section, we discuss the density of states in the framework of RG. The scaling of the DOS is $\rho(E) \propto E^{d_n/z-1}$.[29] For the clean system ($z = 1$), we obtain $\rho_0(E) = I_n E^{2/n}$. In the presence of disorder, we use the approximation of weak disorder $1/z \approx 1-\Delta$, and the RG equation of the density of states is

$$\frac{d\rho}{d\ln E} = \left(\frac{2}{n} - d_n\Delta_n\right)\rho. \quad (10)$$

In order to solve this equation, we first introduce the quasiparticle residue Z, the flow equation is defined as $\frac{dZ}{d\ln E} = \Delta(E)Z$,[41] and the solution is obtained by direct integration,

$$Z(E) = \begin{cases} \sqrt{1-2\Delta_2\ln(\Lambda/E)}, & (n=2), \\ \sqrt{1+6\Delta_3(1-(\Lambda/E)^{1/3})}, & (n=3). \end{cases} \quad (11)$$

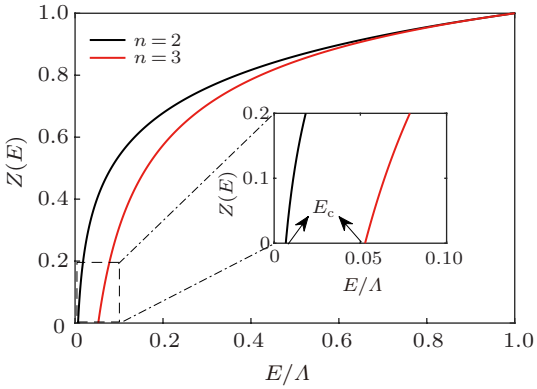


Fig. 2. The quasiparticle residue Z_E of double (black line) and triple (red line) WSMs as a function of energy E/Λ. The inset shows the behavior of Z_E around the low energy cut-off E_c.

In both disorder and interacting fermion systems, the quasiparticle residue plays a decisive role. We plot the quasiparticle residue Z_E as a function of energy in Fig. 2, the value of Z_E for double WSM is smaller than that of triple WSM, which indicates that the influence of disorder is stronger in triple WSM. Now we can express the solution of Eq. (10) in terms of the quasiparticle residue as $\rho = \rho_0 Z^{-d_n}$ and we find

$$\rho(E) = \begin{cases} \frac{I_2 E}{1-2\Delta_2\ln(\Lambda/E)}, & (n=2), \\ \frac{I_3 E^{2/3}}{(1-6\Delta_3[(\Lambda/E)^{\frac{1}{3}}-1])^{5/6}}, & (n=3). \end{cases} \quad (12)$$

Because the inverse of the quasiparticle residue is always larger than unity, the low-energy density of states of the disordered multi WSM is larger than that of the disorder-free system (ρ_0), therefore, the disorder has transferred states from high energies to lower energies.[25] At high energies ($E \to \Lambda$), the quasiparticle residue is close to unity, $Z(E) \approx 1$, and the density of states returns to that of the clean system ρ_0. By expanding the dominator of Eq. (12) as $\frac{1}{1-x} \approx 1+x$, we find that the leading correction to the density of states is proportional to $E\ln(\Lambda/E)$[40] for double WSM and is $E^{2/3}(\Lambda/E)^{1/3}$ for triple WSM, which is in agreement with the calculation of SCBA (we present the results in Appendix A).

The quasiparticle residue $Z(E)$ vanishes as the energy reaches the low energy cut-off E_c (see, Fig. 2), and the one loop RG breaks down. Thus, equation (12) is only valid for

$E \gg E_c$. As long as the strength of disorder is weak, the result obtained by the RG flow equation is always applicable. For $E < E_c$, the density of states approaches to a finite value which can be estimated by SCBA as

$$\rho = -\frac{2}{\pi\gamma}\mathrm{Im}\Sigma\ (E=0) = \begin{cases} \dfrac{2I_2\Lambda e^{-\frac{1}{\Delta_2}}}{\pi\Delta_2}, & (n=2), \\ 2I_3\pi^2\Lambda^{2/3}(\Delta_3)^2, & (n=3). \end{cases} \tag{13}$$

Any finite amount of disorder will generate a finite value of density of states at the nodal point and cause instability of mWSM. Now we turn to discuss the renormalization of the classical conductivity.

4. Renormalization of conductivity

Let us start from calculating the dc conductivity at zero temperature. By using the Kubo formula,[25,45] the conductivity at Fermi energy E is given by

$$\sigma_{\mu\mu}(E) = \frac{e^2}{2\pi}\int \frac{d^3k}{(2\pi)^3}\mathrm{Tr}\left(j_\mu \hat{G}^R(k,\omega) j_\mu \hat{G}^A(k,\omega)\right), \tag{14}$$

where G^R and G^A are the retarded and advanced Green functions,

$$G^{R/A}(E,\boldsymbol{k}) = \frac{1}{E^{R/A} - H_n(\boldsymbol{k})}. \tag{15}$$

We define $E^{R/A} = E \pm \frac{i}{2\tau}$ and the relaxation time τ is determined from the Fermi's golden rule, $1/\tau = \pi\gamma\rho$. The velocity operator is defined as $j_\mu = \partial_{k_\mu} H_n(k)$,

$$j_x = n v_\parallel (k_-^{n-1}\sigma_+ + k_+^{n-1}\sigma_-), \quad j_z = v_z\sigma_z. \tag{16}$$

Plugging these expressions into the Kubo formula and completing the angle integration, we obtain the conductivity along the k_x direction

$$\sigma_{xx}(E) = \frac{n}{6\pi^3 v_z}\int dk \frac{(3E^2-k^2)k^2}{[(E^R)^2-\varepsilon_k^2][(E^A)^2-\varepsilon_k^2]} = \frac{v_x^2}{I_n\gamma} = \begin{cases} \dfrac{E}{3v_z\pi^2 I_2\gamma}, & (n=2), \\ \dfrac{E^{4/3}}{2v_z\pi^2 I_3\gamma}, & (n=3), \end{cases} \tag{17}$$

where we set $e^2 = 1$ for simplicity. Here we define the group velocity along the x direction as $v_x^2 = \frac{nE^{2(1-1/n)}}{6\pi^2 v_z}$ (see Appendix B). For double WSM, because of the quadratic energy dispersion along the x direction, the conductivity σ_{xx} exhibits the behavior of conventional 2D Schrodinger electron gas[18] which is a linear function with Fermi energy E_F,[43] and for triple WSM, σ_{xx} is proportional to $E_F^{4/3}$ due to the cubic dispersion relation. The same results can be obtained for the y direction, where $\sigma_{yy} = \sigma_{xx}$.

Along the direction of linear dispersion k_z, there is a nonzero vertex correction to the velocity operator j_z, which can be calculated by the Bethe–Salpeter equation[44]

$$\tilde{j}_z = j_z + \langle \hat{V}\hat{G}^R\tilde{j}_z\hat{G}^A\hat{V}\rangle. \tag{18}$$

We solve the above equation through the ladder approximation and define $\tilde{j}_z = j_z\Pi$, then we have

$$\tilde{j}_z = j_z + \gamma\int \frac{d^3p}{(2\pi)^3} G^R(p)\tilde{j}_z(p)G^A(p). \tag{19}$$

The integration of the second term on the right hand side is

$$v_z\Pi\gamma\int \frac{d^3p}{(2\pi)^3} G^R(p)\sigma_z(p)G^A(p) = \begin{cases} v_z\Pi\gamma I_2\displaystyle\int dp \frac{pE^2}{[(E^R)^2-\varepsilon_p^2][(E^A)^2-\varepsilon_p^2]}\sigma_z, & (n=2), \\ v_z\Pi\gamma\dfrac{I_3}{5}\displaystyle\int dp \frac{p^{2/3}(5E^2+p^2)}{[(E^R)^2-\varepsilon_p^2][(E^A)^2-\varepsilon_p^2]}\sigma_z, & (n=3) \end{cases} = \begin{cases} \dfrac{v_z}{2}\Pi\sigma_z, & (n=2), \\ \dfrac{3v_z}{5}\Pi\sigma_z, & (n=3). \end{cases} \tag{20}$$

Using Eq. (19), we obtain the vertex correction to the velocity operator,

$$\tilde{j}_z = \begin{cases} 2j_z, & (n=2), \\ \dfrac{5}{2}j_z, & (n=3). \end{cases} \tag{21}$$

Then, the classical conductivity along the k_z direction is given by

$$\sigma_{zz} = \begin{cases} \dfrac{v_z^2}{\pi\gamma}, & (n=2), \\ \dfrac{3v_z^2}{2\pi\gamma}, & (n=3). \end{cases} \tag{22}$$

Notice that σ_{zz} is independent of the Fermi energy. However, due to the renormalization of disorder coupling Δ, one can expect that the conductivity σ_{zz} is reduced as the Fermi energy decreases.[25,40] In order to obtain the analytical result, using the scaling relation $\frac{\sigma_{zz}(E)}{\sigma_{zz}} \sim (\frac{E}{\Lambda})^{1-2/n}\frac{\Delta_n}{\Delta_n(E)}$ and Eq. (8), we obtain

$$\sigma_{zz}(E) = \begin{cases} \dfrac{v_z^2}{\pi\gamma}\left[1 - 2\Delta_2\ln\left(\dfrac{\Lambda}{E}\right)\right], & (n=2), \\ \dfrac{3v_z^2}{2\pi\gamma}\left[1 - 6\Delta_3\left[\left(\dfrac{\Lambda}{E}\right)^{\frac{1}{3}} - 1\right]\right], & (n=3). \end{cases} \tag{23}$$

The first term in Eq. (23) is the constant classical conductivity in Eq. (22), the second term is the correction due to the renormalization of the quasiparticle. For double WSM, the logarithmic correction to the classical conductivity is reminiscent of the transport behavior of Dirac fermion.[39,40] Equation (23) can also be interpreted as the renormalization of

group velocity $\tilde{v}_z(E) = v_z Z(E)$ (see Fig. 2), then we can rewrite Eq. (23) as $\sigma_{zz}(E) \propto \tilde{v}_z^2/\gamma$. Thus, the renormalization of quasiparticle property gives an important correction to the transport behavior of the system. Using the similar procedure, we can calculate the modification of σ_{xx} by replacing $\tilde{v}_x(E) = v_x Z(E)$ in Eq. (16).

As the energy approaches to the low energy cut-off E_c, the one-loop RG breaks down. Here, we estimate the conductivity below the energy scale E_c by evaluating the Kubo–Greenwood formula[45]

$$\sigma_{\mu\mu}(E_F) = e^2 \int \frac{d^3k}{(2\pi)^3} \mathrm{Tr}(j_\mu \hat{A}(k,\omega) v_\mu \hat{A}(k,\omega)). \quad (24)$$

The spectral operator $\hat{A}$ is defined as $\hat{A}(k,\omega) = (\hat{G}^R - \hat{G}^A)/(2i)$, equation (24) can be calculated under the eigen space (Eq. (2)), we present the details in Appendix A and the final results are

$$\begin{aligned} \sigma_{xx}^{n=2}(E \to 0) &= \frac{\eta}{2\pi^2 v_z}, \\ \sigma_{zz}^{n=2}(E \to 0) &= I_2 v_z^2, \\ \sigma_{xx}^{n=3}(E \to 0) &= \frac{3\eta}{4\pi^2 v_z}, \\ \sigma_{zz}^{n=3}(E \to 0) &= \frac{I_3 v_z^2}{3\eta^{1/3}}, \end{aligned} \quad (25)$$

where we define $\eta = |\mathrm{Im}\Sigma|$. Around the nodal point, for both double and triple WSMs, the conductivity along the x direction is proportional to the imaginary part of self energy $\sigma_{xx} \propto \eta$. For triple WSM, using the result $\mathrm{Im}\Sigma(0) = -\Lambda(\pi\Delta_3)^3$ in Appendix A, the conductivity along z direction is controlled by $\sigma_{zz}^{n=3} \propto 1/\Delta_3$. However, for double WSM, the $\sigma_{zz}^{n=2}$ at the nodal point is independent of disorder, which is similar to the universal conductivity[33] of graphene at the Dirac point.

5. Conclusion

In summary, we investigate the quasiparticle and transport behavior of weakly disordered double and triple Weyl fermions. We show that the density of states is enhanced in the presence of disorder and the diffusive conductivity is renormalized. More interestingly, the constant classical conductivity along the z direction is substantially corrected due to the renormalization of quasiparticle residue Z_E. The energy dependence of σ_{zz} gives an unconventional temperature dependence $\sigma_{zz}(T)$ and can be directly measured by experiments.

Appendix A: Self-consistent Born approximation

The disorder averaged self energy matrix from the Born approximation is $\hat{\Sigma}(E) = \overline{\langle \hat{V}\hat{G}(E)\hat{V}\rangle}$, where the Green's function contains the self energy, and forms a self-consistent loop,

$$\Sigma_n(E) = \frac{W^2}{12} \int \frac{d^3k}{(2\pi)^3} \frac{E - \Sigma(E) - H_n(\boldsymbol{k})}{(E-\Sigma(E))^2 - \varepsilon_k^2},$$

$$= I_n \gamma \int k^{2/n} dk \frac{E - \Sigma(E)}{(E-\Sigma(E))^2 - k^2}. \quad (A1)$$

For double WSM ($n = 2$), we obtain

$$\Sigma_{n=2}(E) = -I_2 \frac{\gamma}{2} [E - \Sigma(E)] \ln \frac{-\Lambda^2}{[E-\Sigma(E)]^2}. \quad (A2)$$

By setting $E = 0$, we find that the imaginary part of the self-energy contains a constant term at the nodal point, $\mathrm{Im}\Sigma(E = 0) = -\Lambda e^{-\frac{1}{I_2\gamma}}$, which has the same order as the small energy scale E_c in Eq. (9). In the high energy limit $E \gg E_c$, we obtain the result of the first order Born approximation, $\mathrm{Im}\Sigma(E) = -\frac{\pi}{2} I_2 \gamma E$, a simple iteration gives the next order correction, and we have

$$\mathrm{Im}\Sigma_{n=2}(E) = \begin{cases} -\Lambda e^{-\frac{1}{\Delta_2}}, & E < E_c, \\ -\dfrac{\pi}{2}\Delta_2 E(1 + \Delta_2 \ln(\Lambda/E)), & E \gg E_c. \end{cases} \quad (A3)$$

Using the same logic, we find the solution for triple WSM ($n = 3$),

$$\begin{aligned} &\mathrm{Im}\Sigma_{n=3}(E) = -\pi(-1)^{1/6}\gamma I_3 (E - \Sigma(E))^{2/3} \\ &= \begin{cases} -\Lambda(\pi\Delta_3)^3, & E < E_c, \\ -\dfrac{\pi}{2}\Lambda^{1/3}\Delta_3 E^{2/3}\left(1 + \dfrac{2}{\sqrt{3}}\Delta_3\left(\dfrac{\Lambda}{E}\right)^{1/3}\right), & E \gg E_c. \end{cases} \end{aligned} \quad (A4)$$

Once the equation is solved, the density of states be expressed by the imaginary part of the self energy

$$\rho(E) = -\frac{2}{\pi\gamma}\mathrm{Im}\Sigma(E). \quad (A5)$$

Appendix B: Kubo–Greenwood formula

We express the longitudinal conductivity using Kubo–Greenwood formula

$$\sigma_{\mu\mu}(E_F) = \int \frac{d^3k}{(2\pi)^3} \mathrm{Tr}(j_\mu \hat{A}(k,\omega) j_\mu \hat{A}(k,\omega)), \quad (B1)$$

where the operator $\hat{A}$ is defined as $\hat{A}(k,\omega) = (\hat{G}^R - \hat{G}^A)/(2i)$ which is diagonal under the eigen bases Eq. (2),

$$A(k,\omega) = \begin{pmatrix} A_+(k,\omega) & 0 \\ 0 & A_-(k,\omega) \end{pmatrix}, \quad (B2)$$

where $A_\pm(k,\omega) = \frac{\eta}{(E \mp \varepsilon_k)^2 + \eta^2}$ is the spectral function of the Weyl Fermion, and $\eta = |\mathrm{Im}\Sigma|$. The trace can be calculated under the eigen-spaces,

$$\langle +|j_x|+\rangle = -\langle -|j_x|-\rangle = n v_\parallel \left(\frac{k\sin\theta}{v_\parallel}\right)^{\frac{n-1}{n}} \sin\theta\cos\phi,$$

$$\langle +|j_x|-\rangle = \langle -|j_x|+\rangle^* = n v_\parallel \left(\frac{k\sin\theta}{v_\parallel}\right)^{\frac{n-1}{n}} (i\sin\phi + \cos\theta\cos\phi),$$

$$j_z = v_z \begin{pmatrix} \cos\theta & -\sin\theta \\ -\sin\theta & -\cos\theta \end{pmatrix}. \tag{B3}$$

We first calculate the angle average

$$\overline{|\langle s|j_\mu|s'\rangle|^2} = \frac{1}{(2\pi)^3}\int_0^\pi \mathrm{d}\theta \int_0^{2\pi} \mathrm{d}\phi \frac{\csc\theta(\sin\theta)^{2/n}}{n v_\parallel^{2/n} v_z} |\langle s|j_\mu|s'\rangle|^2,$$

$$\overline{|\langle +|j_x|+\rangle|^2} = \overline{|\langle -|j_x|-\rangle|^2} = \frac{nk^{2(1-1/n)}}{6v_z\pi^2},$$

$$\overline{|\langle +|j_x|-\rangle|^2} = \overline{|\langle -|j_x|+\rangle|^2} = \frac{nk^{2(1-1/n)}}{3v_z\pi^2},$$

$$\overline{|\langle +|j_z|+\rangle|^2} = \overline{|\langle -|j_z|-\rangle|^2} = \frac{nv_z^2 I_n}{(2+n)},$$

$$\overline{|\langle +|j_z|-\rangle|^2} = \overline{|\langle -|j_z|+\rangle|^2} = \frac{2v_z^2 I_n}{(2+n)}. \tag{B4}$$

After completing the trace, we arrive at

$$\sigma_{xx}^{n=2}(E) = \int \mathrm{d}k \frac{k^2}{3v_z\pi^2}(A_+^2 + 4A_+A_- + A_-^2),$$

$$\sigma_{zz}^{n=2}(E) = \int \mathrm{d}k \frac{kI_2 v_z^2}{2}(A_+^2 + 2A_+A_- + A_-^2),$$

$$\sigma_{xx}^{n=3}(E) = \int \mathrm{d}k \frac{k^2}{2v_z\pi^2}(A_+^2 + 4A_+A_- + A_-^2),$$

$$\sigma_{zz}^{n=3}(E) = \int \mathrm{d}k \frac{k^{2/3} I_3 v_z^2}{5}(3A_+^2 + 4A_+A_- + 3A_-^2). \tag{B5}$$

Around the band touching point $E = 0$, the integration over the momentum k then leads to Eq. (25).

References

[1] Lv B Q, Xu N, Weng H M, Ma J Z, Richard P, *et al.* 2015 *Nat. Phys.* **11** 724
[2] Xu S Y, Belopolski I, Alidoust N, Neupane M, Zhang C, *et al.* 2015 *Science* **349** 613
[3] Wang H C and Wang J 2018 *Chin. Phys. B* **27** 107402
[4] Xu S Y, Alidoust N, Belopolski I, Zhang C, Bian G, *et al.* 2015 *Nat. Phys.* **11** 748
[5] Son D T and Spivak B Z 2013 *Phys. Rev. B* **88** 104412
[6] Burkov A A 2014 *Phys. Rev. Lett.* **113** 187202
[7] Lu H Z and Sheng S Q 2016 *Chin. Phys. B***25**, 117202
[8] Sun L and Wan S L 2015 *Chin. Phys. Lett.* **32** 057501
[9] Xu G, Weng H, Wang Z, Dai X and Fang Z 2011 *Phys. Rev. Lett.* **107** 186806
[10] Fang C, Gilbert M J, Dai X and Bernevig B A 2012 *Phys. Rev. Lett.* **108** 266802
[11] Huang S M, Xu S Y, Belopolski I, Lee C C, Chang G, *et al.* 2016 *Proc. Natl. Acad. Sci. USA* **113** 1180
[12] Liu Q H and Zunger A 2017 *Phys. Rev. X* **7** 021019
[13] Mai X Y, Zhang D W, Li Z and Zhu S L 2017 *Phys. Rev. A* **95** 063616
[14] Lepori L, Fulga I C, Trombettoni A and Burrello M 2016 *Phys. Rev. A* **94** 053633
[15] Roy B, Goswami P and Juricic V 2017 *Phys. Rev. B* **95** 201102(R)
[16] Lai H H 2015 *Phys. Rev. B* **91** 235131
[17] Zhang S X, Jian S K and Yao H 2017 *Phys. Rev. B* **96** 241111(R)
[18] Chen Q and Fiete G A 2016 *Phys. Rev. B* **93** 155125
[19] Park S, Woo S, Mele E J and Min H 2017 *Phys. Rev. B* **95** 161113(R)
[20] Ahn S, Mele E J and Min H 2017 *Phys. Rev. B* **95** 161112(R)
[21] Mukherjee S P and Carbotte J P 2018 *Phys. Rev. B* **97** 045150
[22] Gorbar E V, Miransky V A, Shovkovy I A and Sukhachov P O 2017 *Phys. Rev. B* **96** 155138
[23] Goswami P and Chakravarty S 2011 *Phys. Rev. Lett.* **107** 196803
[24] Syzranov S V, Radzihovsky L and Gurarie V 2015 *Phys. Rev. Lett.* **114** 166601
[25] Syzranov S V, Ostrovsky P M, Gurarie V and Radzihovsky L 2016 *Phys. Rev. B* **93** 155113
[26] Pixley J H, Goswami Pallab and Sarma S Das 2015 *Phys. Rev. Lett.* **115** 076601
[27] Fu B, Zhu W, Shi Q, Li Q, Yang J, and Zhang Z 2017 *Phys. Rev. Lett.* **118** 146401
[28] Sbierski B, Trescher M, Bergholtz E J and Brouwer P W 2017 *Phys. Rev. B* **95** 115104
[29] Bera S, Sau J D and Roy B 2016 *Phys. Rev. B* **93** 201302(R)
[30] Lee P A and Ramakrishnan T V 1985 *Rev. Mod. Phys.* **57** 287
[31] Ioffe A F, and Regel A R 1960 *Prog. Semicond.* **4** 237
[32] Imry Y 2002 *Introduction to Mesoscopic Physics* (Oxford: Oxford University Press)
[33] Castro Neto A H, Guinea F, Peres N M R, Novoselov K S and Geim A K 2009 *Rev. Mod. Phys.* **81** 109
[34] Altland A 2006 *Phys. Rev. Lett.* **97** 236802
[35] Song H D, Sheng D, Wang A Q, Li J G, Yu D P and Liao Z M 2017 *Chin. Phys. B* **26** 037301
[36] Wang L M, Shi S C and Zhang W Y 2013 *Chin. Phys. B* **22** 127201
[37] Nersesyan A A, Tsvelik A M and Wenger F 1994 *Phys. Rev. Lett.* **72** 2628
[38] Nersesyan A A, Tsvelik A M and Wenger F 1995 *Nucl. Phys. B* **438** 561
[39] Aleiner I L, and Efetov K B 2006 *Phys. Rev. Lett.* **97** 236801
[40] Ostrovsky P M, Gornyi I V and Mirlin A D 2006 *Phys. Rev. B* **74** 235443
[41] Zhao P L, Wang J R, Wang A M and Liu G Z 2016 *Phys. Rev. B* **94** 195114
[42] Isobe H, Yang B J, Chubukov A, Schmalian J and Nagaosa N 2016 *Phys. Rev. Lett.* **116** 076803
[43] Banerjee S and Pickett W E 2012 *Phys. Rev. B* **86** 075124
[44] Shon N H and Ando T 1998 *J. Phys. Soc. Jpn* **67** 2421
[45] Akkermans E and Montambaux G 2007 *Mesoscopic Physics of Electrons and Photons* (Cambridge: Cambridge University Press)